



# Hydriding and dehydriding kinetics of RbH-doped 2LiNH<sub>2</sub>/MgH<sub>2</sub> hydrogen storage system



Jalaal Hayes, Tolulope Durojaiye, Andrew Goudy\*

Department of Chemistry, Delaware State University, 1200 N. Dupont Highway, Dover, DE 19901, USA

## ARTICLE INFO

### Article history:

Available online 23 December 2014

### Keywords:

Hydrogen storage  
Lithium amide  
Rubidium hydride  
Absorption kinetics  
Cycling  
Thermodynamics

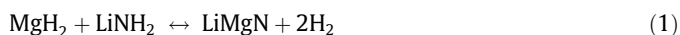
## ABSTRACT

In this study, thermodynamic and kinetic properties of RbH doped 2LiNH<sub>2</sub>/MgH<sub>2</sub> were measured and compared for hydrogen absorption and desorption. Pressure–composition–temperature isotherms were obtained in the 150–180 °C temperature range and were used to construct van't Hoff plots. The results showed that the absorption enthalpy, 39.7 kJ mol<sup>−1</sup>, was less than the desorption enthalpy, 43 kJ mol<sup>−1</sup>. Kinetics measurements, done at 160 °C using constant pressure thermodynamic driving forces, show that under the same conditions, absorption is approximately twice as fast as desorption. Modeling studies, based on a shrinking core model, show that diffusion is the rate-limiting process for both absorption and desorption. Cycling studies were also done to determine if any changes would occur in the sample upon repeated hydriding/dehydriding at 200 °C. It was found that the amount of hysteresis increased and there was also about a 30% decrease in the hydrogen capacity after 70 cycles.

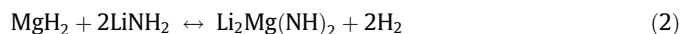
© 2014 Elsevier B.V. All rights reserved.

## 1. Introduction

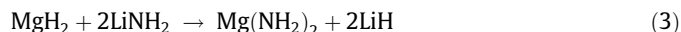
Scientists have been studying the hydrogen sorption properties of numerous metal alloys to see if they would be suitable as hydrogen storage materials. Some of the most promising materials have been amides. In 2002, Chen et al. [1] reported that lithium nitride (Li<sub>3</sub>N) could absorb ~10 wt.% hydrogen reversibly via a two-step reaction. In the first step Li<sub>3</sub>N is converted to an imide (Li<sub>2</sub>NH) and in the second step the imide is converted to an amide (LiNH<sub>2</sub>). Since the hydrogen pressure corresponding to the first step is very low, only the second step involving the reaction of Li<sub>2</sub>NH and LiNH<sub>2</sub>, is considered useful for practical applications. This step has a theoretical hydrogen capacity of 6.5 wt.%. Xiong et al. [2] were able to demonstrate that the addition of Ca or Mg to the binary Li<sub>2</sub>NH to form a ternary Li–Ca–N–H or Li–Mg–N–H system resulted in a significant change in the performance of the system. Their results showed that the ternary systems absorbed and desorbed hydrogen at much lower temperatures than the binary system. Alapati et al. [3] used first principles calculations to predict that the introduction of Mg into the system via the following reaction scheme showed promise for hydrogen storage.



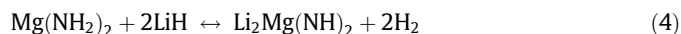
This system has a theoretical hydrogen storage capacity of 8.19 wt.% and DFT calculations showed that the reaction enthalpy was a very favorable 31.9 kJ/mol. Luo [4] ball milled a mixture consisting of 2LiNH<sub>2</sub>/1.1MgH<sub>2</sub> and was able to demonstrate that the imide (Li<sub>2</sub>NH) could be destabilized by the partial substitution of lithium with magnesium via the reaction:



The 10% excess of MgH<sub>2</sub> was used to prevent the amide from decomposing during ball milling. It was demonstrated that the Mg-substituted material had a plateau pressure of ~30 bar at 200 °C and a hydrogen capacity of 4.5 wt.%. Chen et al. [5] did structural analyses which indicated that upon, ball milling, the initial dehydrogenation reaction of 2LiNH<sub>2</sub>/MgH<sub>2</sub> forms a Mg(NH<sub>2</sub>)<sub>2</sub>/LiH phase according to the reaction:



This phase reacted reversibly to form Li<sub>2</sub>Mg(NH)<sub>2</sub> according to the reaction:



They noted that the dehydriding rate of this material decreases markedly upon lowering the operation temperature. Therefore suitable catalysts were needed to enhance the reaction rates. Wang et al. [6] demonstrated that the introduction of KH dopant into the Mg(NH<sub>2</sub>)<sub>2</sub>/LiH phase resulted in the lowering of the desorption temperature from >180 °C for the pristine system to ~107 °C for

\* Corresponding author. Tel.: +1 302 857 6534; fax: +1 302 857 6539.

E-mail addresses: [jalaal.hayes@gmail.com](mailto:jalaal.hayes@gmail.com) (J. Hayes), [tolusko@yahoo.com](mailto:tolusko@yahoo.com) (T. Durojaiye), [agoudy@desu.edu](mailto:agoudy@desu.edu) (A. Goudy).

the doped material. Durojaiye and Goudy [7] did thermodynamics and kinetics measurements on both the KH catalyzed  $\text{LiNH}_2/\text{MgH}_2$  and  $2\text{LiNH}_2/\text{MgH}_2$  systems and found that the  $\text{LiNH}_2/\text{MgH}_2$  material desorbed hydrogen at a lower temperature and with faster kinetics than the  $2\text{LiNH}_2/\text{MgH}_2$  system. However, the KH dopant had very different effects on these systems. The KH markedly decreased the desorption temperature and increased the reaction rate of the  $2\text{LiNH}_2/\text{MgH}_2$  system but it had almost no effect on the  $\text{LiNH}_2/\text{MgH}_2$  material. In another study, Durojaiye et al. [8] reported that RbH was a significantly better catalytic additive for the  $2\text{LiNH}_2/\text{MgH}_2$  system than KH, with desorption rates twice as fast. The rate limiting process for hydrogen desorption was found to be diffusion. However, their studies did not include absorption kinetics. In this study, thermodynamics and kinetics for absorption and desorption of hydrogen from the  $2\text{LiNH}_2/\text{MgH}_2$  system are compared. In addition, the cyclic stability of this system is determined.

## 2. Experimental

All chemicals used in this study were obtained from Sigma Aldrich. The lithium amide ( $\text{LiNH}_2$ ) was 95% pure and magnesium hydride ( $\text{MgH}_2$ ) was 98% pure. Both of these compounds were hydrogen storage grade. The rubidium hydride (RbH) catalyst was synthesized by a mechanical alloying procedure that was described by Durojaiye et al. [8]. A mixture consisting of  $1.9\text{LiNH}_2 + 1.1\text{MgH}_2 + 0.1\text{RbH}$  was prepared by a ball milling procedure. This procedure consisted of placing ~5 g of the mixture in a 65 mL milling vial with 10–20 g stainless steel milling balls. The mixture was ball milled in a SPEX 8000D high-energy mixer/mill for 2 h under an argon atmosphere. Pressure–Composition Isotherms (PCI) were obtained using a Gas Reaction Controller-PCI unit. The instrument was manufactured by the Advanced Materials Corporation. Data for PCI analysis were collected in a range from 150 to 180 °C. Data for cycling studies were collected at a constant temperature at 200 °C. A Lab View based software package was used to view and collect the data.

Kinetic measurements for hydriding and dehydriding were conducted in a stainless steel Sievert's apparatus at 160 °C. In order to assure that all measurements were done at the same constant pressure thermodynamic driving force, the same ratio of mid-plateau region to opposing pressure was used for each measurement. This ratio is defined as the *N*-value. For absorption reactions, the ratio is (opposing pressure/plateau pressure) whereas for desorption reactions the ratio is (plateau pressure/opposing pressure). Further details about the procedures used to obtain constant pressure thermodynamic driving forces have been discussed elsewhere by Goudy and co-workers [7,9,10].

## 3. Results

### 3.1. Pressure Composition Isotherm (PCI) measurements

PCI measurements for the  $1.9\text{LiNH}_2 + 1.1\text{MgH}_2 + 0.1\text{RbH}$  system were conducted in the range from 150 to 180 °C. The results for absorption PCI measurements are shown in Fig. 1a. As expected, each isotherm displays a well-defined plateau region in which lower temperatures result in lower plateau pressures. The isotherms show different maximum weight percent. It can be seen that the weight percent generally increases with increasing temperature. Similar plots were obtained for desorption isotherms. These isotherms were used to construct the van't Hoff plots shown in Fig. 1b. The slopes of these plots were then used to determine enthalpies of absorption and desorption. The values for absorption and desorption enthalpies were found to be 39.7 and 43.0 kJ mol<sup>-1</sup>, respectively. The desorption enthalpy value is similar to that reported by Durojaiye et al. [8] who performed measurements in the 200–230 °C range. We are not aware of any other absorption enthalpies reported for the RbH catalyzed system.

### 3.2. Cycling studies

Fig. 2a contains a pair of absorption and desorption isotherms that were obtained at 200 °C after 20 absorption/desorption cycles. These plots show that there is a significant amount of hysteresis in this system. Fig. 2b contains plots of cycle number vs plateau

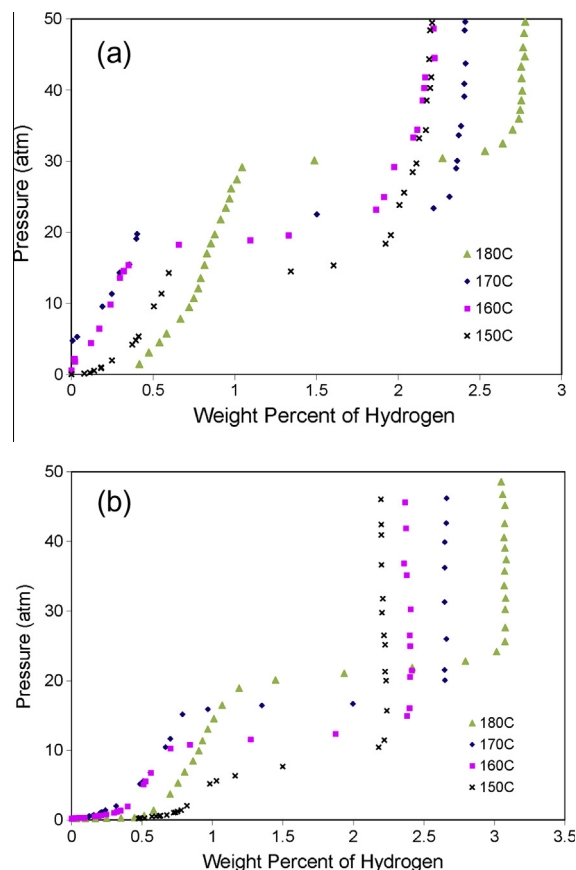


Fig. 1. (a) Absorption PCI measurements for the  $1.9\text{LiNH}_2 + \text{MgH}_2 + 0.1\text{RbH}$  system; and (b) desorption PCI measurements for the  $1.9\text{LiNH}_2 + \text{MgH}_2 + 0.1\text{RbH}$  system.

pressure. The isotherms were measured after every set of 10 absorption/desorption cycles. These show how the absorption and desorption plateau pressures change during pressure/vacuum cycling. It is evident that the absorption plateau pressures gradually increase whereas the desorption pressures decrease during cycling. The difference between the absorption and desorption plateaus prior to cycling was 8 atm. However, this difference increased to 50 atm after 70 cycles. The hydrogen holding capacity also shows about a 30% decrease when going from 0 to 70 cycles.

### 3.3. Kinetics and modeling studies

In order to be of use for many practical applications, a potential hydrogen storage system should undergo hydriding and dehydriding reactions rapidly and reversibly. Therefore kinetics measurements were done and comparisons were made of the absorption and desorption rates of the RbH-doped  $2\text{LiNH}_2/\text{MgH}_2$  system at 160 °C under equivalent conditions. This was accomplished by using an *N*-value of 3 for the hydriding and dehydriding processes. Since the desorption plateau pressure at 160 °C is 12.3 atm, an opposing pressure of 4.1 atm was applied. In the case of absorption, the plateau pressure is 18.2 atm. Therefore a pressure of 54.6 atm was applied. Fig. 3 contains the absorption and desorption kinetics plots of RbH catalyzed  $2\text{LiNH}_2/\text{MgH}_2$  mixtures. The absorption reaction seems to be 90% completed in ~400 min whereas the desorption reaction takes ~800 min. The observed differences in kinetics between desorption and absorption may due to a number of factors such as the nature of the different phase components in two states.

To elucidate the mechanism of these reactions, a shrinking core model was used. This model has been used by Sabitu et al. [11] to

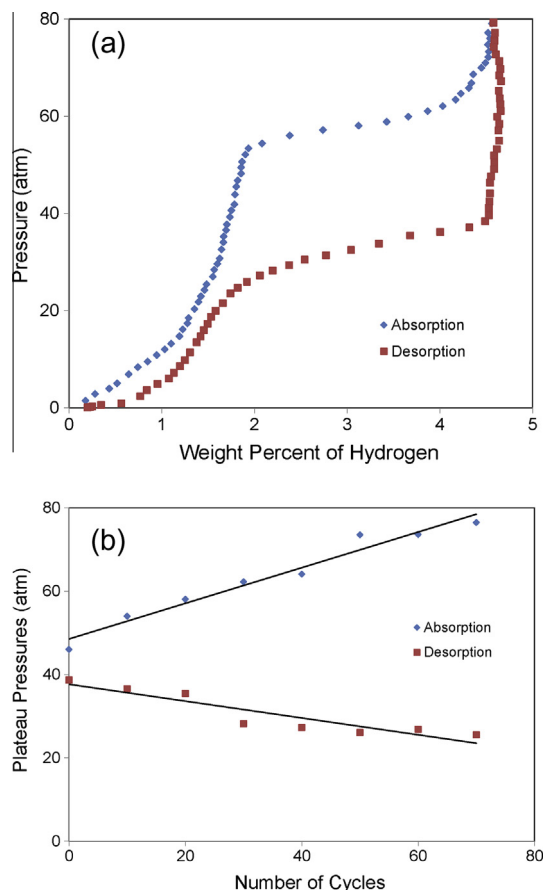


**Fig. 2.** (a) Comparison of absorption and desorption cycling measurement at 200 °C and (b) hysteresis plot of absorption/desorption cycling measurements at 200 °C.

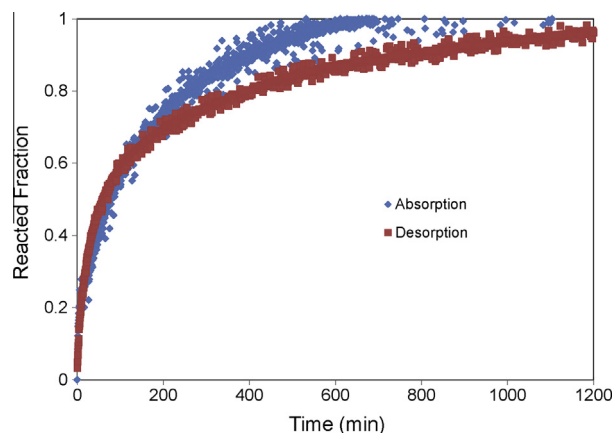


**Fig. 3.** Kinetic plot comparison of absorption and desorption for the 1.9LiNH<sub>2</sub> + -MgH<sub>2</sub> + 0.1RbH system with  $T = 160\text{ °C}$  and  $N$ -value of 3.

describe the desorption kinetics for the magnesium hydride system. It was also used by Durojaiye et al. [8] to describe the desorption kinetics of the lithium amide/magnesium hydride system. In this study, we used this model to describe both desorption and absorption kinetic studies. The equations used to model this system are shown below.

$$\frac{t}{\tau} = 1 - (1 - X_B)^{1/3} \quad (5)$$

$$\frac{t}{\tau} = 1 - 3(1 - X_B)^{2/3} + 2(1 - X_B) \quad (6)$$

where  $t$  is the time at a specific point in the reaction,  $X_B$  is the fraction of the metal reacted and  $\tau$  is a collection of constants. Statistical methods were used to determine a value for  $\tau$  that would minimize the difference between the theoretical and experimental curves. In Eq. (5) chemical reaction at the phase boundary controls the reaction rate whereas in Eq. (6) diffusion controls the rate.

Eqs. (5) and (6) were fitted to the kinetic data in Fig. 3 for the absorption and desorption reactions. Fig. 4a contains three curves for the absorption reaction modeling. One is an experimental curve taken from Fig. 3; a second curve was calculated from Eq. (5) and a third curve was calculated from Eq. (6). The results show that the data generated from the model with diffusion controlling the overall rate fits the experimental data better than the data generated from the model with chemical reaction controlling the overall reaction rate. This is true only during the first 70% of the reaction. During the last 30% of the reaction, neither model was a good fit with the experimental data. The reason for this is that during the first 70% of the reaction, desorption occurred along the plateau region where the pressure remained relatively constant. Therefore the  $N$ -value was constant and thus the thermodynamic driving force was constant. When the reaction reached the left edge of the plateau region the pressure decreased sharply and the thermodynamic driving force decreased. At this point the kinetics slowed more rapidly than either model predicted.

In the case of absorption, it can be seen from Fig. 4b that the data generated from the model with diffusion controlling the overall rate fits the experimental data better than the reaction controlled model. Unlike the desorption case, this curve fits the

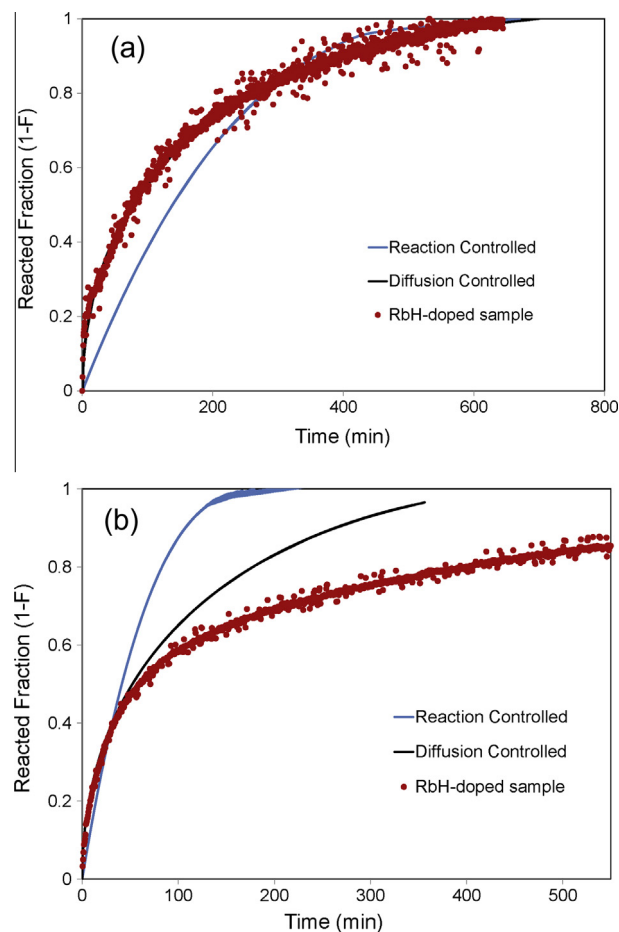


**Fig. 4.** (a) Shrinking core model of RbH-catalyzed system for absorption kinetics and (b) shrinking core model of RbH-catalyzed system for desorption kinetics.

experimental data over virtually the entire course of the reaction. The reason for this can be seen if one examines the isotherms in Fig. 1a. The absorption reaction proceeds along the isotherm from left to right until the end of the plateau is reached on the right side. At this point, the isotherm rises very sharply to the final pressure with a minimal amount of hydrogen being absorbed along the steep rise. Nearly all of the hydrogen is released along the plateau region. This is different than the desorption process in which 30% of the hydrogen was released along the gradual sloping portion of the isotherm.

#### 4. Conclusion

This study has shown that RbH is an effective catalytic additive for increasing the rates of hydrogen absorption and desorption from the  $2\text{LiNH}_2/\text{MgH}_2$  system. Absorption rates are about twice as fast as desorption. Modeling studies indicate that the rates of both absorption and desorption are controlled by a diffusion process. There is also a substantial amount of hysteresis in this system and the magnitude of it increases during the first 70 absorption/

desorption cycles. There is also about a 30% decrease in the storage capacity of this system during the first 70 cycles.

#### Acknowledgments

This research was supported by Grants from the U.S. Department of Energy and the U.S. Department of Transportation.

#### References

- [1] P. Chen, Z. Xiong, J. Luo, J. Lin, K.L. Tan, *Nature* 420 (2002) 302–304.
- [2] Z. Xiong, G. Wu, J. Hu, P. Chen, *Adv. Mater.* 16 (2004) 1522–1525.
- [3] S.V. Alapati, J.K. Johnson, D.S. Sholl, *J. Phys. Chem. B* 110 (2006) 8769–8776.
- [4] W. Luo, *J. Alloys Comp.* 381 (2004) 284–287.
- [5] Y. Chen, C.Z. Wu, P. Wang, H.M. Cheng, *Int. J. Hydrogen Energy* 31 (2006) 1236–1240.
- [6] J. Wang, T. Liu, G. Wu, W. Li, Y. Liu, C. Araujo, R. Scheicher, A. Blomqvist, R. Ahuja, A. Xiong, Z. Xiong, P. Yang, M. Gao, H. Pan, P. Chen, *Angew. Chem., Int. Ed.* 48 (2009) 5828–5832.
- [7] T. Durojaiye, A. Goudy, *Int. J. Hydrogen Energy* 37 (2012) 3298–3304.
- [8] T. Durojaiye, J. Hayes, A. Goudy, *J. Phys. Chem. C* 117 (2013) 6554–6560.
- [9] H. Yang, A. Ojo, P. Ogaro, A.J. Goudy, *J. Phys. Chem. C* 113 (2009) 14512–14517.
- [10] A. Ibikunle, A. Goudy, *Int. J. Hydrogen Energy* 37 (2012) 12420–12424.
- [11] S.T. Sabitu, O. Fagbami, A.J. Goudy, *J. Alloys Comp.* 509S (2011) S588–S591.